Stability and Performance Analysis of an Adaptive Sigma–Delta Modulator

Mansour A. Aldajani, *Student Member, IEEE,* and Ali H. Sayed, *Fellow, IEEE*

***Abstract*—This work develops an adaptive sigma–delta modulator that is based on adapting the quantizer step-size using estimates of the quantizer input rather than the modulator input. The adaptive modulator with a first-order noise shaping filter is shown to be bounded-input bounded-output stable. Moreover, an analytical expression for the signal-to-noise ratio is derived, and it is shown to be independent of the input signal strength. Simulation results confirm the signal-to-noise ratio performance and indicate considerable improvement in the dynamic range of the modulator compared to earlier structures.**

***Index Terms*—Adaptive step-size, dynamic range, quantization, sigma–delta modulation, stability.**

I. Introduction

A. Sigma–Delta Modulation

SIGMA–DELTA modulation (SDM) is used to perform high-resolution analog-to-digital conversion (ADC) using low-complexity components. A general structure for sigma–delta modulation is shown in Fig. 1. An analog signal $x(t)$ is sampled at a rate higher than the Nyquist rate. The sampler is usually preceded by an antialiasing (AA) filter. Since the sampling rate is higher than the Nyquist rate, the design of the AA filter is less constrained. At the modulator, each sample $x(n)$ is converted into a digital value $y(n)$ with a certain number of bits.

In general, the modulator shapes the noise power spectrum by moving it as much as possible outside of the signal bandwidth in order to decrease the in-band noise power. The frequency spectrum of the signal $y(n)$ will then contain the input signal in its low-band portion. The function of the demodulator is to extract the input signal from $y(n)$, usually by means of low-pass filtering. The demodulated signal is still at high rate and thus needs to be decimated to the Nyquist rate. Fig. 2 shows the modulation/demodulation stages of a single-loop (single-stage) SDM. In this example, the modulator consists of a noise shaping filter $H(z)$ and a single-bit quantizer while the demodulator is a low-pass filter. This basic structure has been extended to more efficient structures including multiloop, multistage, and multibit modulators (see, e.g., [1]).

Manuscript received November 2000; revised February 2001. This work was supported in part by by the National Science Foundation under Grant CCR-9732376 and Grant ECS-9820765. The work of M. A. Aldajani was supported by a fellowship from King Fahd University of Petroleum and Minerals, Saudi Arabia. This paper was recommended by Associate Editor R. Geiger.

The authors are with the Department of Electrical Engineering, University of California, Los Angeles, CA 90095 USA.

Publisher Item Identifier S 1057-7130(01)04201-X.

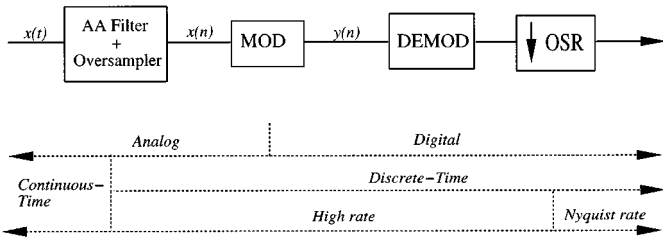

Fig. 1. General structure for sigma–delta modulation.

B. Adaptive Sigma–Delta Modulation

Adaptive sigma–delta modulation (ASDM) attempts to increase the dynamic range of sigma–delta modulators while keeping the quantization noise as low as possible. ASDM achieves this objective by scaling either the input signal or the step-size of the quantizer through an estimation of the input signal strength. This estimation can be done from the input signal itself or from the modulator output, as shown in Fig. 3. Input scaling is shown in Fig. 3(a), while step-size scaling is shown in Fig. 3(b). Using the input signal to perform the estimation is known as forward estimation, while using the output signal is known as backward estimation. Adaptation could be done continuously or sporadically in time. Moreover, the value of the adaptation signal $d(n)$ could be continuous in amplitude or restricted to a specific range of values.

Several adaptation techniques have been investigated in the literature. Chakravarthy [2] proposed an adaptive scheme that is based on averaging the number of transitions at the modulator output. Jaggi and Chakravarthy [3] used a digital-to-analog converter to instantaneously control the feedback pulse amplitude. Yu *et al.* [4] developed a technique based on estimating the maximum input amplitude over a certain interval and using it to adapt the quantization step-size. This work has been extended by Dunn and Sandler [5] to a multibit quantizer. Ramesh and Chao [6] implemented a backward adaptation. In their work, the feedback signal of the modulator is scaled by power-of-two gains based on the estimate of the input amplitude.

In this paper, we develop a new scheme for adapting the quantization step-size. The proposed technique is based on estimating the amplitude of the quantizer input instead of the input signal itself. We perform both stability and performance analysis of the new structure. Based on simulation and analytical results, the new modulator shows considerable improvement in dynamic range and signal-to-noise ratio (SNR) performance.

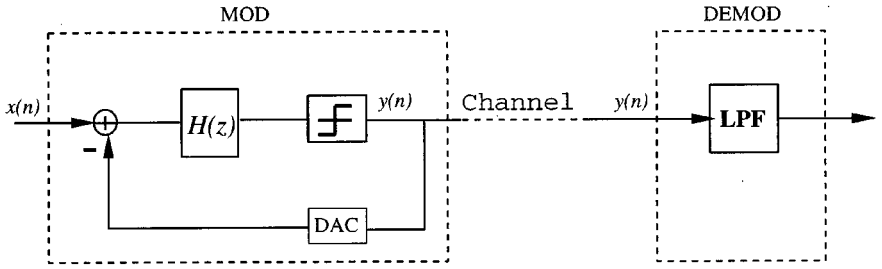

Fig. 2. Modulation/demodulation stages of a single-loop SDM.

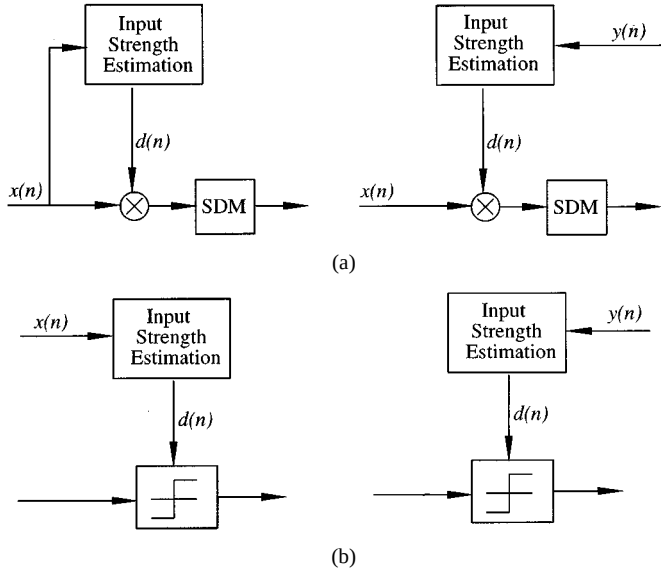

Fig. 3. Adaptation schemes used in conventional ASDMs. (a) Input scaling. (b) Quantizer step-size scaling.

II. A New ASDM Structure

A. Motivation

For the sake of motivation, consider the plot shown in Fig. 4 and assume that we want to construct a signal $v(n)$ that tracks a signal $x(n)$ (e.g., a step signal). This can be achieved according to the following construction. At each instant of time, we start with the value $v(n-1)$ and update it to $v(n)$ so that this new value is closer to $x(n)$ than its old value. The update is based on the difference between $x(n)$ and $v(n-1)$, defined by

$$e_a(n) = x(n) - v(n-1). \tag{1}$$

The signal $v(n-1)$ is increased or decreased by a positive amount $d(n)$ depending on the size and sign of this error. Intuitively, if the error is "large," we employ a large value for the correction term $d(n)$; and if the error is "small," we employ a smaller correction term. More specifically, in our construction, the value of $d(n)$ is made to change by a constant factor α or $1/\alpha$, where $\alpha > 1$. The law by which $d(n)$ varies is chosen as follows:

$$d(n) = \begin{cases} \alpha d(n-1), & \text{if } |e_a(n)| > d(n-1) \\ \dfrac{1}{\alpha} d(n-1), & \text{otherwise.} \end{cases} \tag{2}$$

The sign of the error $e_a(n)$ decides whether $v(n-1)$ increases or decreases at each time instant. Thus, the signal $v(n)$ is varied according to the adaptation rule

$$v(n) = v(n-1) + \text{sign}\,[e_a(n)]\, d(n). \tag{3}$$

Observe that the correction term $d(n)$, also called step-size, can be expressed in the equivalent form

$$d(n) = \alpha^{w(n)}\, d(0) \tag{4}$$

where

$$w(n) = w(n-1) + q(n) \tag{5}$$

and

$$q(n) = \text{sign}\,[|e_a(n)| - d(n-1)]. \tag{6}$$

This alternative representation allows us to describe the scheme for updating $v(n)$ in block diagram form, as shown in Fig. 5. The top and bottom parts of the figure implement (4) and (3), respectively.

The diagram shown in Fig. 5 has the structure of an adaptive delta modulator, with the upper part being the adaptation scheme for the quantizer step-size. The adaptation signal $d(n)$ is tracking the absolute value of the error signal $e_a(n)$. Although this system belongs to the class of adaptive delta modulators (e.g., [7]–[11]), the adaptation technique used here is different (see [12] for more details).

B. Proposed ASDM Structure

Delta modulators do not apply noise shaping and, for this reason, their performance is generally limited. Now since sigma–delta modulators are essentially delta modulators applied to the integral of the input signal [13], [14], the ADM design shown in Fig. 5 suggests an ASDM by moving back the integrator of the main loop to become the first block after the adder.

Fig. 6 shows the basic structure of the resulting adaptive sigma–delta modulator, with a 1-bit quantizer. The modulation and demodulation blocks are shown in Fig. 6(a) and (b), respectively. The integrator is replaced by a general noise-shaping filter $H(z)$.

The error signal $e_a(n)$ is still given by

$$e_a(n) = x(n) - v(n-1) \tag{7}$$

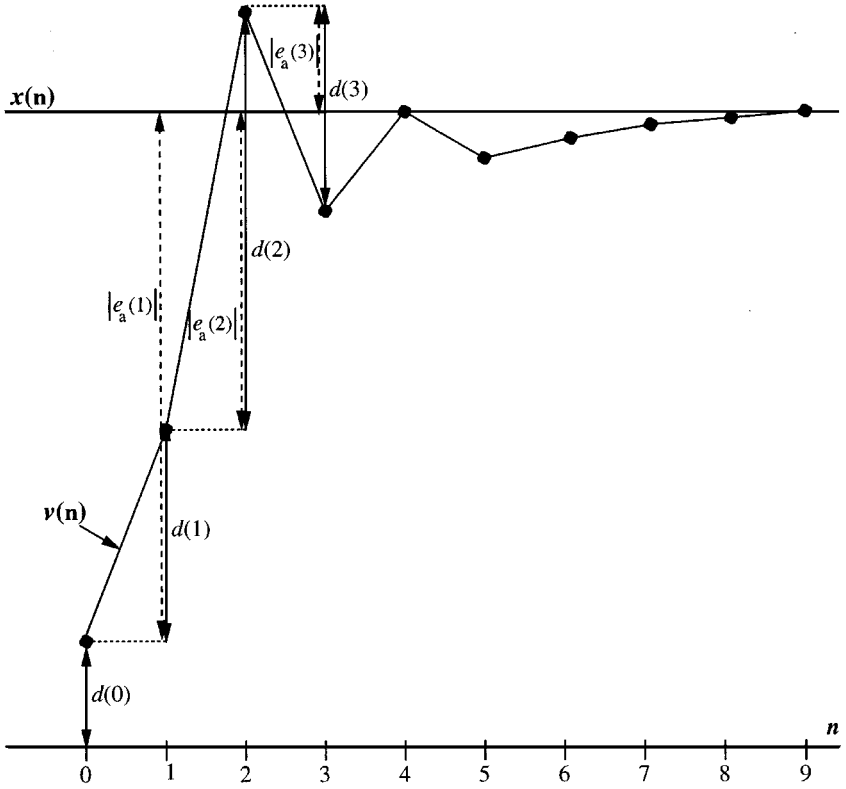

Fig. 4. Response of an output signal $v(n)$ tracking a step input $x(n)$.

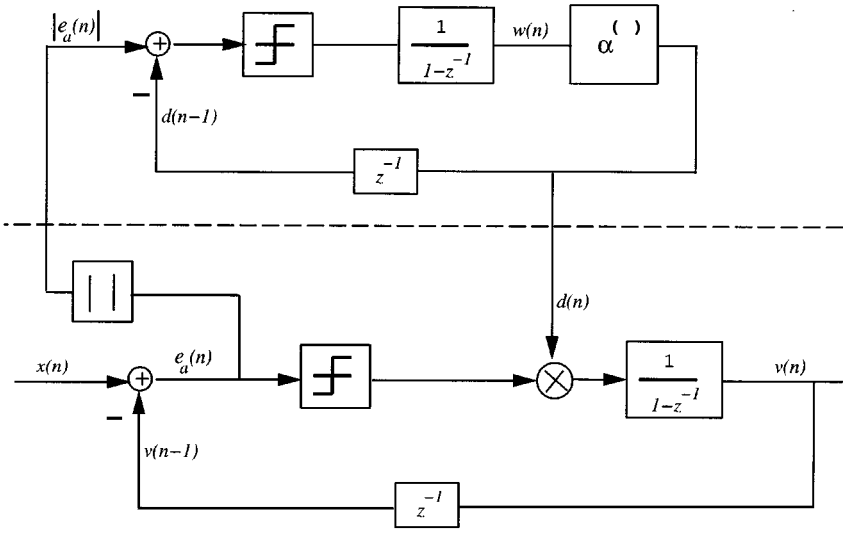

Fig. 5. Adaptive delta modulator.

which is passed through the noise-shaping filter $H(z)$. As a special case, if $H(z)$ is a simple integrator, then

$$p(n) = p(n-1) + e_a(n) \quad \text{with} \quad p(0) = 0. \tag{8}$$

The filter output $p(n)$ is quantized using a 1-bit quantizer to produce the signal $y(n)$. In other words

$$y(n) = \text{sign}\,[p(n)]. \tag{9}$$

The 1-bit digital-to-analog converter (DAC) is assumed to be ideal and thus has a unity transfer function. The adapter generates a scaling signal $d(n)$, which is an approximation of the amplitude of the quantizer input signal $p(n)$. The encoded signal $v(n)$ is then given by

$$v(n) = y(n)\, d(n). \tag{10}$$

Notice that if $d(n) = |p(n)|$, then we would have

$$V(z)/X(z) = 1. \tag{11}$$

The adaptation block for $d(n)$ is shown in Fig. 7, which is similar in structure to a delta modulator with an additional exponent term α. The purpose of this additional term is to increase the tracking capability of the adapter.

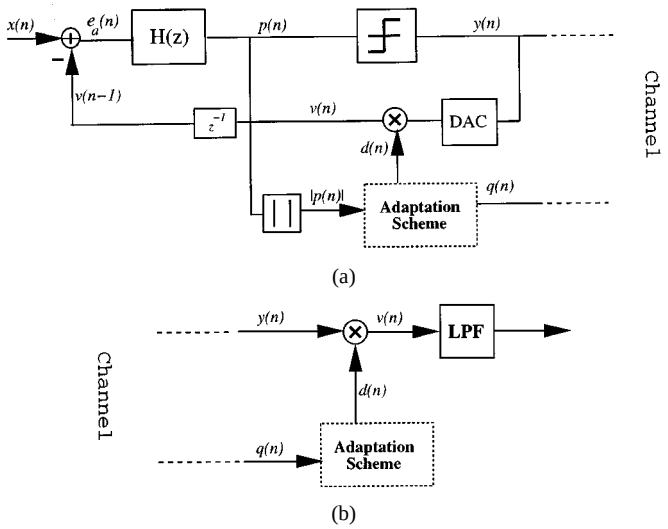

Fig. 6. Block diagram of the proposed structure. (a) Modulator. (b) Demodulator.

The adaptation signal $d(n)$ is therefore constructed as follows:

$$d(n) = \alpha^{q(n)}\, d(n-1) \tag{12}$$

where the binary sequence $q(n)$ is generated from

$$q(n) = \begin{cases} +1, & \text{if } |p(n)| > d(n-1) \\ -1, & \text{otherwise.} \end{cases} \tag{13}$$

In other words

$$q(n) = \text{sign}\,[|p(n)| - d(n-1)]. \tag{14}$$

The two binary sequences $y(n)$ and $q(n)$ are carried out to the demodulation part, as shown in Fig. 6(b). There, the signal $v(n)$ is reconstructed using (12) and (10). Finally, the reconstructed signal is filtered using a low-pass filter, as usually done in conventional sigma–delta modulators.

C. Design Considerations

One way to implement the additional circuitry used in this modulator is by using analog switches. First, the adaptive scheme shown in Fig. 7 can be implemented as illustrated in Fig. 8(a). The signal $d(n)$ is generated from (12) depending on the state of $q(n)$. In other words

$$d(n) = \begin{cases} \alpha d(n-1), & \text{if } q(n) = +1 \\ \dfrac{1}{\alpha} d(n-1), & \text{if } q(n) = -1. \end{cases} \tag{15}$$

In a similar fashion, the absolute value block in Fig. 6 is replaced by a switching device that chooses between a gain of either $+1$ or -1 depending on the sign of $p(n)$, or equivalently the state of $y(n)$. In other words, the switching system implements the following equation:

$$|p(n)| = \begin{cases} +p(n), & \text{if } y(n) = +1 \\ -p(n), & \text{if } y(n) = -1. \end{cases} \tag{16}$$

This process is depicted in Fig. 8(b).

Finally, the multiplier in Fig. 6 multiplies a real signal $d(n)$ with a binary signal $y(n)$. Thus, it can be replaced by a switch controlled by $y(n)$ to keep or invert the sign of $d(n)$ as shown in Fig. 8(c) i.e.,

$$v(n) = \begin{cases} +d(n), & \text{if } y(n) = +1 \\ -d(n), & \text{if } y(n) = -1. \end{cases} \tag{17}$$

III. Analysis of the Proposed Modulator

In the discussions that follow, we shall study the performance of the adaptive sigma–delta modulator of Figs. 6 and 7. The study will involve a stability proof, a mean and variance analysis, and a derivation of an analytic expression for the resulting SNR. The analysis is restricted to the case where $H(z)$ is an integrator as in (8).

A. Equivalent Structure of the Modulator

We first show how the modulator can be redrawn in a more convenient equivalent form via a suitable transformation of variables.

Consider the modulator shown in Fig. 6 with the adapter shown in Fig. 7. Taking the logarithm of both sides of (12) we get

$$\log_\alpha(d(n)) = \log_\alpha(d(n-1)) + q(n). \tag{18}$$

Using the fact that the logarithm is an increasing function, we can write

$$\begin{aligned} q(n) &\equiv \text{sign}\,[|p(n)| - d(n-1)] \\ &= \text{sign}\,[\log_\alpha(|p(n)|) - \log_\alpha(d(n-1))]. \end{aligned}$$

Now let

$$x_d(n) \equiv \log_\alpha(|p(n)|) \tag{19}$$

and

$$y_d(n) \equiv \log_\alpha(d(n)). \tag{20}$$

Then from (18)–(20), we get

$$y_d(n) = y_d(n-1) + \text{sign}\,[x_d(n) - y_d(n-1)]. \tag{21}$$

This dynamic equation characterizes a delta modulator, as illustrated in Fig. 9(a). Its linearized version is shown in Fig. 9(b). Therefore, we can redraw the adapter of Figs. 6 and 7 in an equivalent form utilizing (19)–(21), as shown in Fig. 10. The adaptation block together with the quantizer of the modulator now looks like a log-PCM [15], except that the PCM block is replaced by a delta modulator.

There are three advantages for using the log-DM over the log-PCM in our case. The first advantage is that log-PCM usually requires a multibit DAC after the PCM block, to reconstruct its analog input, introducing a source of nonlinearity in the overall modulator. Clearly, log-DM does not suffer from this problem since the quantizer used inside the DM is single-bit and thus has a linear behavior.

Furthermore, it is found through simulation that the use of log-PCM introduces large tones at the modulator output, especially when the number of PCM levels is small. These tones are usually undesirable when dealing with speech signals. On the

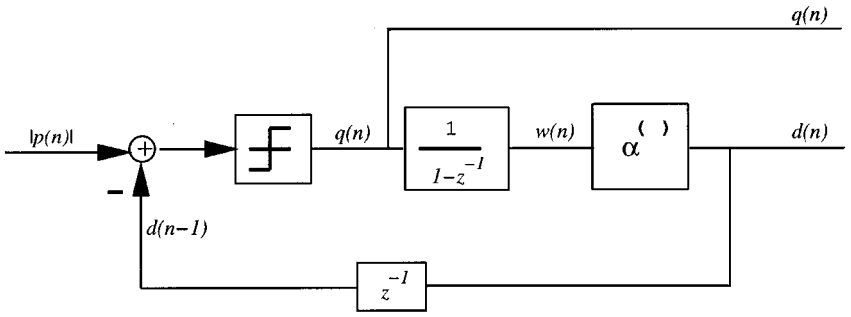

Fig. 7. Adaptation scheme of the proposed modulator.

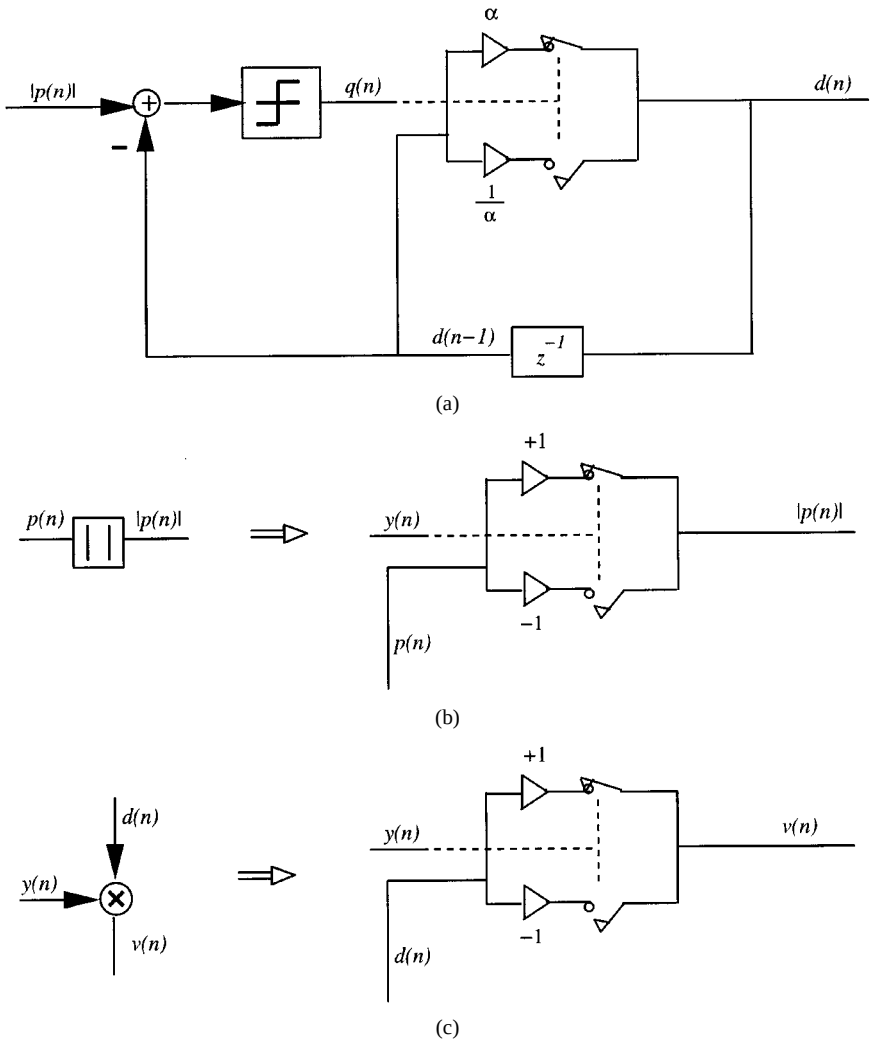

Fig. 8. Implementation of some modulator parts: (a) adaptive scheme, (b) absolute value term, and (c) multiplier.

other hand, the log-DM does not introduce large tones to the modulator since the output of the DM is inherently analog.

Finally, log-PCM offers an SNR performance that is ideally independent of the input signal strength. However, this feature is not practical since it requires a PCM with infinite dynamic range [15]. The log-DM offers practically unlimited dynamic range provided that it is given enough tracking time.

Continuing with our analysis, the delta modulator can be linearized by replacing its quantizer by an additive quantization noise $e_d(n)$, as was shown in Fig. 9(b). The noise $e_d(n)$ is assumed to be uniformly distributed in an interval $[-\Delta, \Delta]$ (usually $\Delta = 1$ for single bit DM). The transfer function of the linearized DM can now be written as

$$Y_d(z) = \frac{\dfrac{1}{1-z^{-1}}}{1+\dfrac{z^{-1}}{1-z^{-1}}}(X_d(z)+E_d(z)) \tag{22}$$

which simplifies to

$$Y_d(z) = X_d(z) + E_d(z). \tag{23}$$

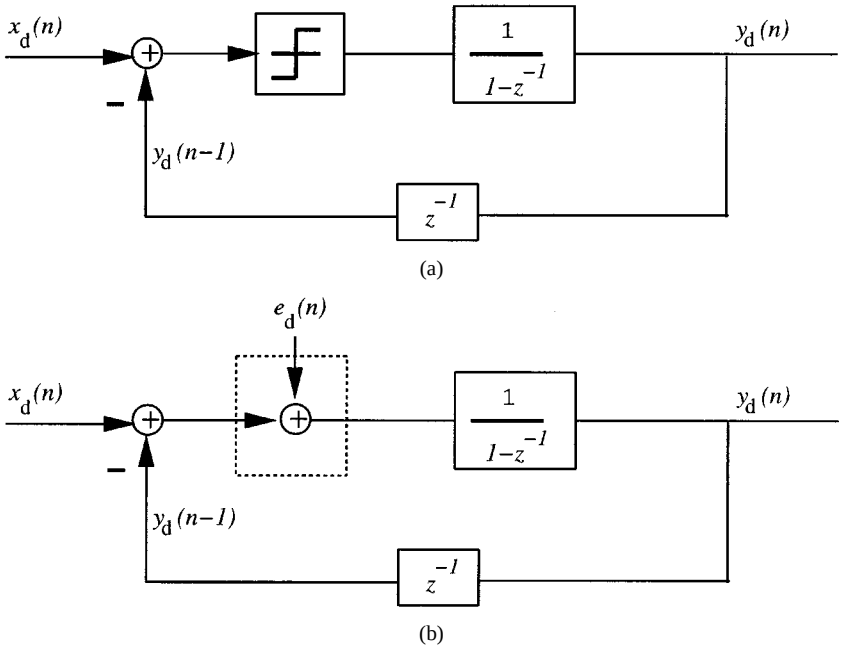

Fig. 9. A Delta modulator. (a) Typical and (b) linearized.

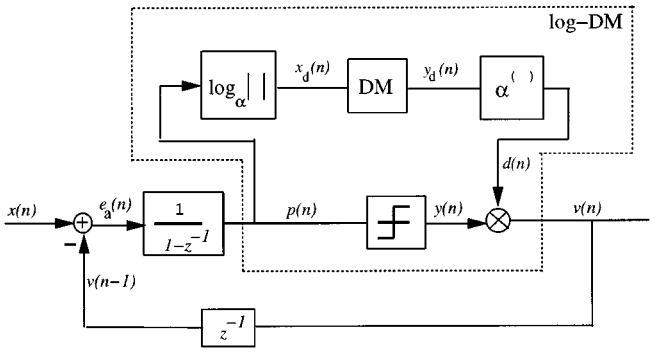

Fig. 10. Equivalent form of the ASDM.

In the time domain, we can write

$$y_d(n) = x_d(n) + e_d(n). \tag{24}$$

Moreover, from (20), we have

$$d(n) = \alpha^{y_d(n)} \tag{25}$$

so that

$$d(n) = \alpha^{x_d(n)+e_d(n)}. \tag{26}$$

Substituting the expression for $x_d(n)$ from (19), we get

$$d(n) = \alpha^{log_\alpha(|p(n)|)+e_d(n)} = |p(n)|\alpha^{e_d(n)}. \tag{27}$$

Substituting back into (3), we have

$$v(n) = p(n)\alpha^{e_d(n)}. \tag{28}$$

Finally, if we denote

$$K(n) \equiv \alpha^{e_d(n)} \tag{29}$$

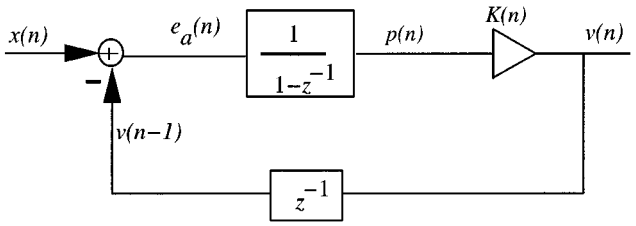

Fig. 11. The ASDM as a linear time-variant (LTV) system.

then we arrive at the expression

$$v(n) = p(n)K(n). \tag{30}$$

This result shows that we can approximate the adapter and quantizer in the main loop of Fig. 6(a) by a time-varying gain $K(n)$. Fig. 11 shows the resulting equivalent structure of our ASDM with first-order noise-shaping filter. Since the distribution of the random error signal $e_d(n)$ is known, the distribution of the variable gain $K(n)$ can be defined. Our further analysis is based on the following assumptions.

1) All random processes are assumed stationary.
2) The variable $K(n)$ is assumed independent of all other variables.

B. Bounded-Input Bounded-Output (BIBO) Stability of the Modulator

Consider the modulator structure shown in Fig. 11. The signal $p(n)$ is given by

$$p(n) = p(n-1) + x(n) - v(n-1). \tag{31}$$

Now from (30), we have

$$p(n) = p(n-1) + x(n) - K(n-1)p(n-1). \tag{32}$$

Thus, the dynamic equation for the signal $p(n)$ can be expressed as

$$p(n) = (1 - K(n-1))p(n-1) + x(n). \tag{33}$$

Since $p(0) = 0$, the forced response of $p(n)$ is

$$p(n) = \sum_{i=1}^{n} \prod_{j=i}^{n} (1 - K(j-1))x(i). \tag{34}$$

When the input signal $x(n)$ is bounded, i.e.,

$$|x(n)| \leq \Lambda < \infty \tag{35}$$

for some Λ, then we get

$$|p(n)| \leq \Lambda \sum_{i=1}^{n} \prod_{j=i}^{n} |1 - K(j-1)|. \tag{36}$$

Lemma 1—BIBO Stability : The signal $p(n)$ will be bounded if

$$|1 - K(n)| \leq L < 1 \tag{37}$$

for some L and for all n. In this case, the modulator output will be bounded by

$$|v(n)| \leq \alpha^{\Delta} \frac{\Lambda}{1-L}. \tag{38}$$

Proof: If (37) is satisfied, i.e., if the quantity $1-K(n)$ is uniformly bounded by 1, then from (36) we conclude that

$$|p(n)| \leq \Lambda \sum_{i=1}^{n} L^{n-i} = \Lambda \sum_{j=0}^{n-1} L^{j} \tag{39}$$

so that

$$|p(n)| \leq \frac{\Lambda}{1-L}. \tag{40}$$

Also, from (30), we conclude that

$$|v(n)| \leq \max_{K(n)} \frac{\Lambda}{1-L}. \tag{41}$$

Referring to (29), the maximum of $K(n)$ is given by

$$\max_{K(n)} = \alpha^{\Delta}. \tag{42}$$

Substituting back into (41), we get

$$|v(n)| \leq \alpha^{\Delta} \frac{\Lambda}{1-L}. \tag{43}$$

■

To complete the argument, we need to show when condition (37) is satisfied. In other words, we need to determine the range of values for the exponent term α such that the quantity $|1 - K(n)|$ is uniformly bounded by one.

1) Corollary—(Choice of α): Assume that $e_d(n)$ is a uniformly distributed random variable between $[-\Delta, \Delta]$. If α is chosen such that

$$2^{-(1/\Delta)} < \alpha < 2^{1/\Delta} \tag{44}$$

then a bound L can be found that satisfies condition (37).

Proof: Let $L = 1 - \epsilon$, where ϵ is a sufficiently small positive number. Then we can write

$$-1 + \epsilon \leq 1 - K(n) \leq 1 - \epsilon. \tag{45}$$

Therefore

$$\epsilon \leq K(n) \leq 2 - \epsilon. \tag{46}$$

Since $K(n) = \alpha^{e_d(n)}$ and $e_d(n)$ is a uniform random variable between$[-\Delta, \Delta]$, then we can write

$$-\epsilon \leq [\alpha^{-\Delta}, \alpha^{\Delta}] \leq 2 - \epsilon. \tag{47}$$

In other words, the closed interval $[\alpha^{-\Delta}, \alpha^{\Delta}]$ lies entirely inside the interval $[-\epsilon, 2-\epsilon]$. Solving for α, we get

$$(2-\epsilon)^{-(1/\Delta)} \leq \alpha \leq (2-\epsilon)^{1/\Delta}. \tag{48}$$

Since this inequality is true for any small $\epsilon > 0$, then

$$2^{-(1/\Delta)} < \alpha < 2^{1/\Delta}. \tag{49}$$

■

C. Mean Analysis

In this section, we show that the input signal $x(n)$ and the output signal $v(n)$ have the same mean. As a result, the error signal $e_a(n)$ has zero mean. To show this, let us take the expected value of both sides of (33)

$$E\{p(n)\} = E\{(1 - K(n-1))p(n-1) + x(n)\}. \tag{50}$$

Based on the independence and stationarity assumptions, we can write

$$E_p = (1 - E_K)E_p + E_x. \tag{51}$$

Here we are writing E_p to denote $Ep(n)$; likewise for E_K and E_x. Solving for E_p, we get

$$E_p = \frac{E_x}{E_K}. \tag{52}$$

We also know from (30) that

$$E\{v(n)\} = E\{K(n)p(n)\}. \tag{53}$$

Therefore

$$E_v = E_K E_p. \tag{54}$$

Substituting (52) for E_p, we get

$$E_v = E_x \tag{55}$$

and consequently

$$E_{ea} = 0 \tag{56}$$

Thus, we conclude that for arbitrary stationary inputs, the expected value of the error signal $e_a(n)$ is zero.

D. Variance Analysis

We now derive an expression for the variance of the error signal $e_a(n)$, which will be used in the next section to derive an expression for the SNR of the modulator.

Consider again (33). If we square both sides, we get

$$p^2(n) = (1-K(n-1))^2 p^2(n-1) + x^2(n) + 2(1-K(n-1))p(n-1)x(n).$$

Based on the independence and stationarity assumptions, the second moment of $p(n)$ is

$$E\{p^2(n)\} = E\{(1-K(n-1))^2\}E\{p^2(n-1)\} + E\{x^2(n)\} + 2E\{(1-K(n-1))\}E\{p(n-1)x(n)\}.$$

Therefore

$$E_{p^2} = (1 - 2E_K + E_{K^2})E_{p^2} + E_{x^2} + 2(1-E_K)E_{px}. \quad (57)$$

Lemmma 2—Cross Correlation: The term E_{px} is given by

$$E_{px} = \frac{1}{E_K} E_{x^2}. \quad (58)$$

Proof: Start from (33) and multiply both sides by $x(n)$

$$p(n)x(n) = (1-K(n-1))p(n-1)x(n) + x(n)x(n). \quad (59)$$

Taking the expected value of both sides yields

$$E\{p(n)x(n)\} = E\{(1-K(n-1))\}E\{p(n-1)x(n)\} + E\{x(n)x(n)\}.$$

For high oversampling ratios (OSRs), $x(n) \simeq x(n-1)$, and thus we can approximate

$$E\{p(n-1)x(n)\} \simeq E\{p(n-1)x(n-1)\} = E_{px}. \quad (60)$$

Therefore

$$E_{px} = (1-E_K)E_{px} + E_{x^2}. \quad (61)$$

Solving for E_{px}, we get

$$E_{px} = \frac{1}{E_K} E_{x^2}. \quad (62)$$

■

Substituting (58) into (57) and collecting terms, we get

$$(2E_K - E_{K^2})E_{p^2} = \frac{2-E_K}{E_K} E_{x^2} \quad (63)$$

i.e.,

$$E_{p^2} = \Psi E_{x^2} \quad (64)$$

with

$$\Psi = \frac{2-E_K}{E_K(2E_K - E_{K^2})}. \quad (65)$$

Also, from the relation between $v(n)$ and $p(n)$ in (30), we get

$$E_{v^2} = E_{K^2}E_{p^2} = \Psi E_{K^2}E_{x^2}. \quad (66)$$

Lemma 3—Error Variance: The error variance $\sigma_{e_a}^2$ can be expressed as

$$\sigma_{e_a}^2 = \sigma_v^2 - \sigma_x^2. \quad (67)$$

Proof: By definition

$$\begin{aligned}\sigma_{e_a}^2 &\equiv E\{e_a(n)^2\} - (E\{e_a(n)\})^2 \\ &= E\{e_a(n)^2\} \\ &= E\{(x(n) - v(n-1))^2\} \\ &= E\{x^2(n) - 2v(n-1)x(n) + v^2(n-1)\}.\end{aligned}$$

Equivalently

$$\sigma_{e_a}^2 = E\{x^2(n)\} - 2E\{v(n-1)x(n)\} + E\{v^2(n-1)\}. \quad (68)$$

However

$$\begin{aligned}E\{v(n-1)x(n)\} &= E\{K(n-1)p(n-1)x(n)\} \\ &= E_K E\{p(n-1)x(n)\} \\ &= E_{x^2}.\end{aligned}$$

Substituting into (68), we get

$$\begin{aligned}\sigma_{e_a}^2 &= E_{v^2} - E_{x^2} \\ &= (E_{v^2} - E_v^2) - (Ex^2 - E_x^2).\end{aligned}$$

Therefore

$$\sigma_{e_a}^2 = \sigma_v^2 - \sigma_x^2. \quad (69)$$

■

Since the means of $v(n)$ and $x(n)$ are equal, we get

$$\sigma_{e_a}^2 = E_{v^2} - E_{x^2}. \quad (70)$$

Using (66), we get

$$\sigma_{e_a}^2 = (\Psi E_{K^2} - 1)E_{x^2}. \quad (71)$$

If the input is zero mean, then

$$\sigma_{e_a}^2 = (\Psi E_{K^2} - 1)\sigma_x^2. \quad (72)$$

E. SNR Computation

At the receiver side, the signal $v(n)$ is filtered using a low-pass filter with cutoff frequency f_c equal to the input signal bandwidth f_B. The modulation error is computed by comparing the filtered signal to the input signal $x(n)$, as shown in Fig. 12(a).

Since $f_c = f_B$, we can introduce an identical filter at the summer end connected to the input $x(n)$ in Fig. 12(a) assuming ideal filtering. Using linearity, the two filters are moved after the summer, resulting in the equivalent form shown in Fig. 12(b).

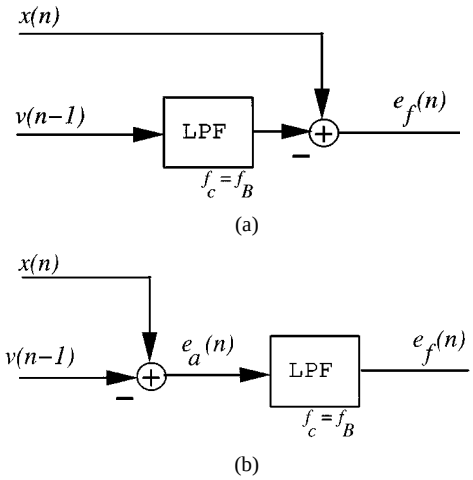

Fig. 12. Modulation error. Two equivalent forms.

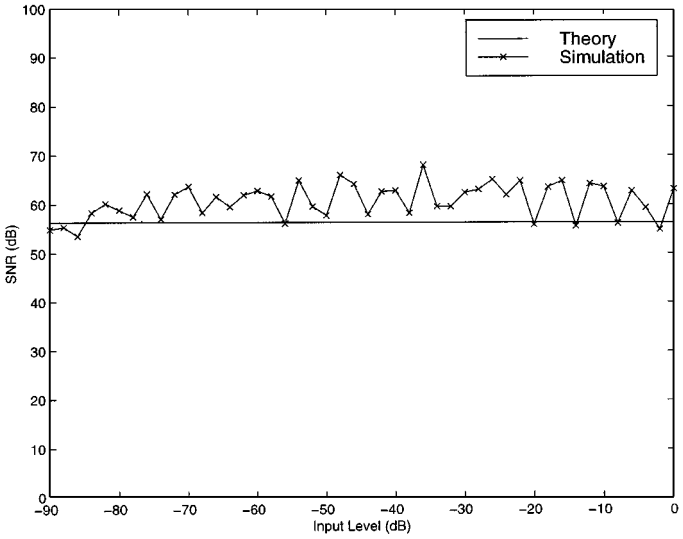

Fig. 13. Comparison between the theoretical and simulated SNR for a first-order noise-shaping filter.

This form is useful in computing the SNR performance of the modulator as follows.

The SNR is defined as the ratio between the input signal variance and the filtered error variance $e_f(n)$ shown in Fig. 12, i.e.,

$$\text{SNR} = \frac{\sigma_x^2}{\sigma_{e_f}^2}. \tag{73}$$

The variance of the filtered error $e_f(n)$ is computed by integrating the spectrum of the error $e_a(n)$ over the input signal bandwidth. For this purpose, we first evaluate the autocorrelation sequence of $e_a(n)$ as follows. Since $e_a(n) = x(n) - v(n-1)$ and $v(n) = K(n)p(n)$, then the dynamics of the error $e_a(n)$ is given by

$$e_a(n) = x(n) - K(n-1)p(n-1). \tag{74}$$

Using (8), we can write

$$p(n) = \sum_{i=0}^{n} e_a(i). \tag{75}$$

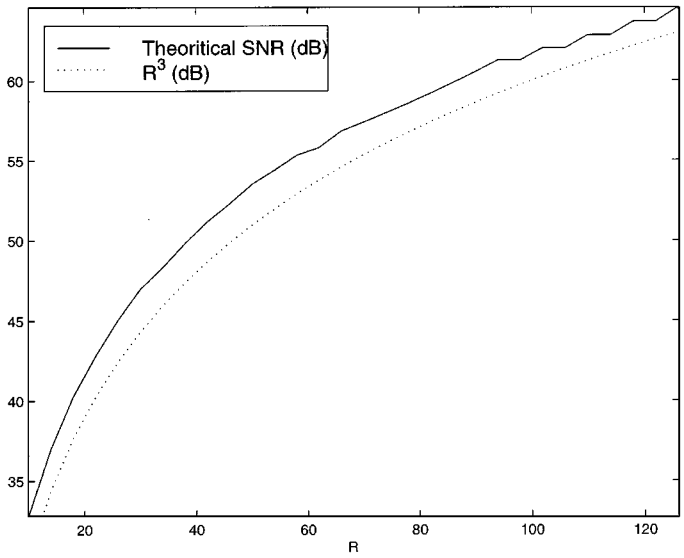

Fig. 14. Theoretical SNR as a function of the oversampling ratio.

Substituting into (74), we get

$$e_a(n) = x(n) - K(n-1) \sum_{i=0}^{i=n-1} e_a(i). \tag{76}$$

Multiplying both sides by $e_a(m)$, $m < n$, yields

$$e_a(n)e_a(m) = x(n)e_a(m) - K(n-1) \sum_{i=0}^{n-1} e_a(i)e_a(m). \tag{77}$$

The expected value of the term $e_a(n)e_a(m)$ is

$$E\{e_a(n)e_a(m)\} = E\{x(n)e_a(m)\} - E\{K(n-1)\}E \cdot \left\{ \sum_{i=0}^{n-1} e_a(i)e_a(m) \right\}.$$

Since the input $x(n)$ is independent of the previous errors $e_a(m), m < n$, then

$$E\{x(n)e_a(m)\} = 0. \tag{78}$$

Therefore

$$E\{e_a(n)e_a(m)\} = -E\{K(n-1)\} \sum_{i=0}^{n-1} E\{e_a(i)e_a(m)\}. \tag{79}$$

Since the process $e_a(n)$ is assumed stationary, its autocorrelation sequence, denoted by γ_{e_a}, satisfies

$$\gamma_{e_a}(n-m) = -E_K \sum_{i=0}^{n-1} \gamma_{e_a}(i-m). \tag{80}$$

In matrix form, we can write, say, for M coefficients

$$A\Gamma_{e_a} = -\mathbf{1}\sigma_{e_a}^2 \tag{81}$$

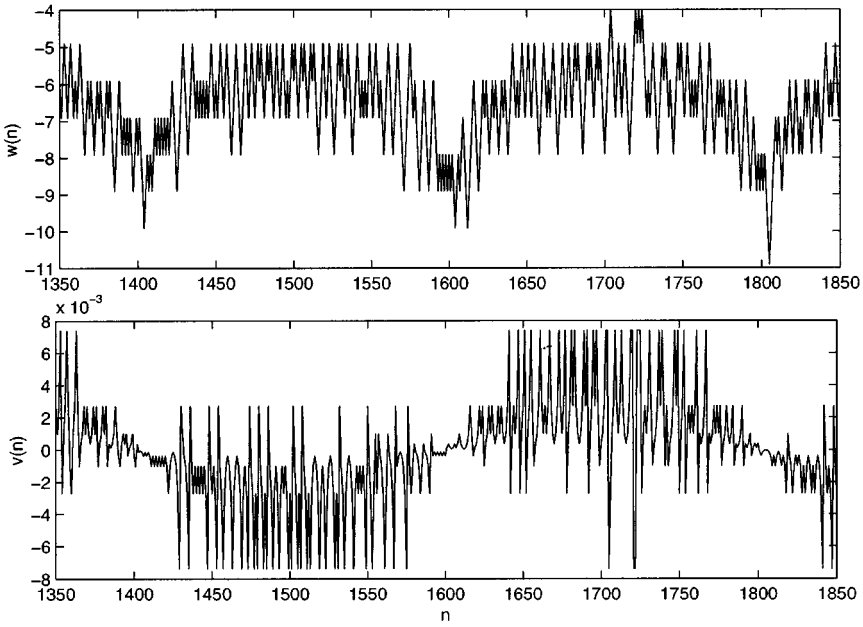

Fig. 15. The signals $w(n)$ and $v(n)$ in time domain for input amplitude of -50 dB.

where

$$A=\begin{pmatrix} 1+\beta & 1 & 1 & \cdots & 1 \\ 2 & 1+\beta & 1 & \cdots & 1 \\ 2 & 2 & 1+\beta & \cdots & 1 \\ \cdot & \cdot & \cdot & \cdots & \cdot \\ \cdot & \cdot & \cdot & \cdots & \cdot \\ 2 & 2 & 2 & \cdots & 1+\beta \end{pmatrix}; \ (M\times M) \quad (82)$$

$$\mathbf{1}=[1 \quad 1 \quad 1 \quad \cdots \quad 1]^T; \qquad (M\times 1)$$

$$\beta=\frac{1}{E_K} \quad (83)$$

and Γ_{e_a} is the vector containing the autocorrelation sequence

$$\Gamma_{e_a}=[\gamma_{e_a}(1) \quad \gamma_{e_a}(2) \quad \cdots \quad \gamma_{e_a}(M)]^T. \quad (84)$$

Solving for Γ_{e_a}, we get

$$\Gamma_{e_a}=-A^{-1}\mathbf{1}\sigma_{e_a}^2. \quad (85)$$

By definition, the spectrum of the error signal $e_a(n)$ is

$$S_{e_a}(w)\equiv\sum_{m=-\infty}^{\infty}\gamma_{e_a}(m)e^{-jw}. \quad (86)$$

But since the sequence γ_{e_a} is real and symmetric, it follows that

$$S_{e_a}(w)=2\sum_{m=1}^{\infty}\gamma_{e_a}(m)\cos(wm)+\gamma_{e_a}(0). \quad (87)$$

In addition, recall that the variance of the filtered error $e_f(n)$ is obtained by integrating the spectrum of $e_a(n)$ over the input frequency bandwidth w_B, i.e.,

$$\sigma_{e_f}^2=\frac{1}{2\pi}\int_{-w_B}^{w_B}S_{e_a}(w)\,dw. \quad (88)$$

We thus arrive at the following result.

Lemma 4—Variance of Filtered Error: Based on the assumption that

$$\gamma_{e_a}(m)=0 \quad \text{for} \quad m>M$$

it holds that

$$\sigma_{e_f}^2=2f_B(1-2S_c^T(w_B)A^{-1}\mathbf{1})\sigma_{e_a}^2 \quad (89)$$

where

$$S_c^T(w_B)=\left[\frac{\sin(w_B)}{w_B} \quad \frac{\sin(2w_B)}{2w_B} \quad \cdots \quad \frac{\sin(Mw_B)}{Mw_B}\right].$$

Proof: Substituting (87) into (88) gives

$$\sigma_{e_f}^2=\frac{1}{\pi}\sum_{m=1}^{M}\gamma_{e_a}(m)\int_{-w_B}^{w_B}\cos(wm)\,dw+\frac{1}{2\pi}\int_{-w_B}^{w_B}\gamma_{e_a}(0)\,dw.$$

Further simplifications result in

$$\sigma_{e_f}^2=\frac{1}{\pi}\sum_{m=1}^{M}\gamma_{e_a}(m)\frac{2}{m}\sin(w_Bm)+\frac{1}{\pi}\gamma_{e_a}(0)w_B. \quad (90)$$

Consequently

$$\sigma_{e_f}^2=\frac{w_B}{\pi}(\gamma_{e_a}(0)+2S_c^T(w_B)\Gamma_{e_a}) \quad (91)$$

where

$$S_c^T(w_B)=\left[\frac{\sin(w_B)}{w_B} \quad \frac{\sin(2w_B)}{2w_B} \quad \cdots \quad \frac{\sin(Mw_B)}{Mw_B}\right].$$

Since $\Gamma_{e_a}=-A^{-1}\mathbf{1}\sigma_{e_a}^2$ and $w_B=2\pi f_B$, then

$$\sigma_{e_f}^2=2f_B(1-2S_c^TA^{-1}\mathbf{1})\sigma_{e_a}^2. \quad (92)$$

■

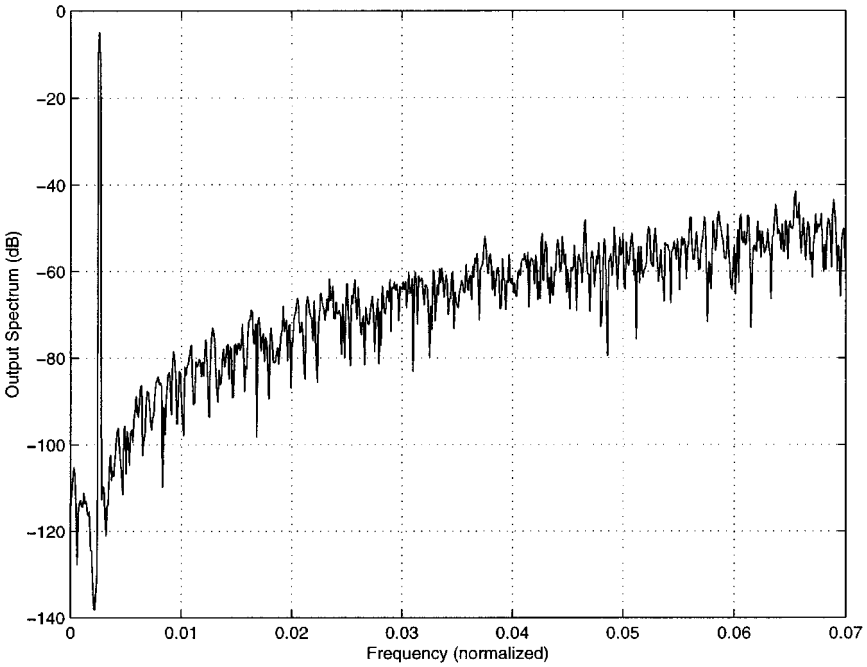

Fig. 16. Spectrum of the modulator output $v(n)$.

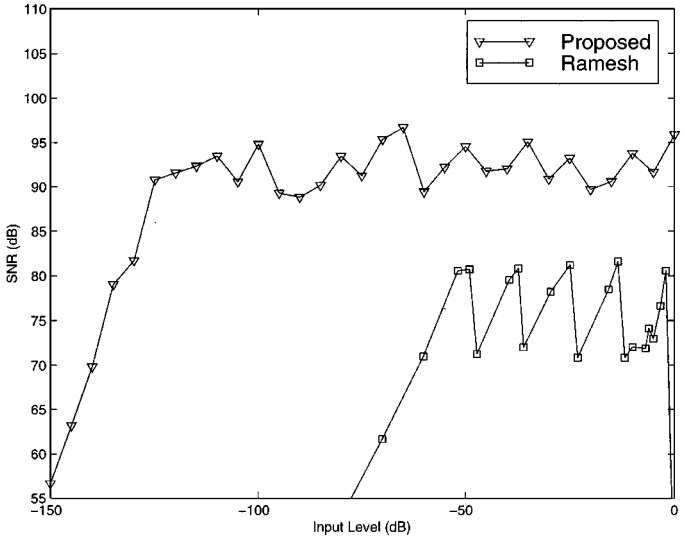

Fig. 17. SNR performance versus input level for the single stage ASDM with second-order noise-shaping filter.

If we now substitute (72) into (89), we get

$$\sigma_{e_f}^2 = 2f_B(1 - 2S_c^T A^{-1}\mathbf{1})(\Psi E_{K^2} - 1)\sigma_x^2 \tag{93}$$

which leads to the SNR expression

$$\text{SNR} = \frac{R}{(1 - 2S_c^T A^{-1}\mathbf{1})(\Psi E_{K^2} - 1)} \tag{94}$$

where R is the OSR.

The above theoretical SNR is clearly independent of the input variance. Fig. 13 shows a comparison between the theoretical and simulated SNR. The figure shows a close relation between them for sinewave input amplitudes as far down as -90 dB.

The SNR is a nonlinear function of the oversampling ratio. Fig. 14 shows the SNR as a function of the oversampling ration R. The SNR changes in the order of R^3 or 30 dB per octave change in the oversampling ratio.

IV. Simulations

The new adaptive sigma–delta modulator is tested via simulation using Matlab and Simulink. The input signal used in the simulation is a sinewave with a frequency of 20 KHz. An OSR of 128 is used and the initial condition for the adaptation signal $d(0)$ is picked arbitrarily small at 1E-3. The noise-shaping filter $H(z)$ used is the second-order filter

$$H(z) = \frac{z^2 - 2z + 1}{z^2 - 1.225z + 0.4415}.$$

The time-domain responses for the signals $w(n)$ and $v(n)$ are shown in Fig. 15 when the amplitude of the input signal is -50 dB. Fig. 16 shows the spectrum of the modulator output $v(n)$ for input amplitude of -5 dB. The amplitude of the input signal is varied and the in-band SNR is measured. The results are plotted in Fig. 17 together with the results obtained in [6] for the sake of comparison. The proposed adaptation scheme shows a superior dynamic range performance.

V. Conclusion

A new adaptive sigma–delta modulator is proposed and analyzed. The adaptation scheme is based on approximating the amplitude of the quantizer input rather than the input to the modulator. The modulator with first-order noise-shaping filter is shown to be BIBO stable, and an expression for the SNR is derived. Simulations have confirmed that the new modulator leads to a high dynamic range performance.

REFERENCES

[1] P. Aziz, H. Sorensen, and J. Spiegel, "An overview of sigma-delta converters," *IEEE Signal Processing Mag.*, vol. 13, pp. 61–84, Jan. 1996.

[2] C. Chakravarthy, "An amplitude controlled adaptive delta sigma modulators," *Radio Electron. Eng.*, vol. 49, no. 1, pp. 49–54, Jan. 1979.

[3] M. Jaggi and C. Chakravarthy, "Instantaneous adaptive delta sigma modulator," *Can. Electr. Eng. J.*, vol. 11, no. 1, pp. 3–6, Jan. 1986.

[4] J. Yu, M. Sandler, and R. Hwaken, "Adaptive quantization for one bit delta sigma modulation," *Proc. Inst. Elect. Eng. Circuits, Devices, Syst.*, vol. 139, no. 1, pp. 39–44, Feb. 1992.

[5] C. Dunn and M. Sandler, "Fixed and adaptive sigma-delta modulator with multibit quantizers," *Appl. Signal Processing*, vol. 3, no. 4, pp. 212–222, 1996.

[6] M. Ramesh and K. Chao, "Sigma delta analog to digital converters with adaptive quantization," in *Proc. IEEE Midwest Symp. Circuits Syst.*, vol. 1.2, 1998, pp. 22–25.

[7] S. Hall and H. Bradlow, "Comparison of 1-bit adaptive quantisers for speech coding," *Electron. Lett.*, vol. 25, no. 9, pp. 586–588, Apr. 1989.

[8] C. Zierhofer, "Numerical adaptive delta modulation—A technique for digital signal representation," in *Proc. IEEE 6th Mediterranean Electrotechnical Conf.*, Ljubljana, Slovenia, May 22–24, 1991, pp. 331–334.

[9] S. Zhang and G. Lockhart, "Design and simulation of an efficient adaptive delta modulation embedded coder," *Proc. Inst. Elect. Eng. Vis. Image Signal Process.*, vol. 142, no. 3, pp. 155–160, June 1995.

[10] Y. Zhu, S. Leung, and C. Wong, "A digital audio processing system based on nonuniform sampling delta modulation," *IEEE Trans. Consumer Electron.*, vol. 42, pp. 80–86, Feb. 1996.

[11] P. Lallo, "Analysis and measurements of information transmission over an adaptive delta modulated voice channel," in *Proc. IEEE MILCOM*, vol. 2, Monterey, CA, Nov. 2–5, 1997, pp. 1057–1061.

[12] M. A. Aldajani and A. H. Sayed, "A stable structure for delta modulation with improved performance," in *Proc. ICASSP*, Salt Lake City, UT, May 2001.

[13] S. Hein and A. Zakhor, *Sigma Delta Modulators*. Boston, MA: Kluwer Academic, 1993.

[14] R. Norsworthy and G. Temes, *Delta-Sigma Data Converters: Theory, Design, and Simulation*. New York: IEEE Press, 1996.

[15] J. Proakis and D. Manolakis, *Digital Signal Processing, Principles, Algorithms, and Applications*. Englewood Cliffs, NJ: Prentice-Hall, 1996.

Mansour A. Aldajani (S'96) received the B.S. and M.S. degrees in systems engineering from King Fahd University of Petroleum and Minerals, Dhahran, Saudi Arabia, in 1994 and 1996, respectively. He is currently working toward the Ph.D. degree in electrical engineering at the University of California, Los Angeles.

His research interests include digital signal processing, adaptive systems, and intelligent networks with applications to control and communications.

Ali H. Sayed (S'90–M'92–SM'99–F'01) received the Ph.D. degree in electrical engineering from Stanford University, Stanford, CA, in 1992.

He is an Associate Professor of electrical engineering at the University of California, Los Angeles. He is Coauthor of the research monograh *Indefinite Quadratic Estimation and Control* (Philadelphia, PA: SIAM, 1999) and of the graduate-level textbook *Linear Estimation* (Englewood Cliffs, NJ: Prentice-Hall, 2000). He is also Coeditor of *Fast Reliable Algorithms for Matrices with Structure* (Philadelphia, PA: SIAM, 1999). He is a member of the editorial boards of the *SIAM Journal on Matrix Analysis and its Applications* and the *International Journal of Adaptive Control and Signal Processing*. He has served as Coeditor of special issues of *Linear Algebra and its Applications*. He has contributed several articles to engineering and mathematical encyclopedias and handbooks and has served on the program committees of several international meetings. He has also consulted to several companies in the areas of adaptive filtering, adaptive equalization, and echo cancellation. His research interests span several areas, including adaptive and statistical signal processing, filtering and estimation theories, equalization techniques for communications, interplays between signal processing and control methodologies, and fast algorithms for large-scale problems. He has published widely in these areas in archival journals and conference proceedings.

Prof. Sayed is an Associate Editor of the IEEE TRANSACTIONS ON SIGNAL PROCESSING. He received the 1996 IEEE Donald G. Fink Award.